Journal of Structural Geology, Vol. 6, No. 5, pp. 449 to 458, 1984
Printed in Great Britain

0191-8141/84 $03.00 + 0.00

Transpression

DAVID J. SANDERSON and W. R. D. MARCHINI

Department of Geology, The Queen's University, Belfast BT7 1NN, U.K.

(*Received* 23 *May* 1983; *accepted in revised form* 18 *November* 1983)

Abstract—Transpression is considered as a wrench or transcurrent shear accompanied by horizontal shortening across, and vertical lengthening along, the shear plane. A model for the strain in transpression is derived, from which the shape and orientation of the finite strain ellipsoid, and the stretch and rotation of lines can be determined. Shortening across the zone of transpression leads to oblate finite strain ellipsoids ($k < 1$).

By considering the superposition of small increments of strain various model deformation paths are computed. These are used to interpret the development of structures, such as en-échelon folds, in transpression zones. The incremental strain ellipsoid allows prediction of the orientation of the principal stresses and hence brittle structures within such zones. The model is also applied to bends and terminations of shear zones and used to interpret the observed patterns of folds and fractures in these.

INTRODUCTION

MANY zones of deformation in the crust are bounded by steep, parallel planes, often representing strain discontinuities manifest as faults or shear zones. If there has been negligible vertical displacement between the rocks on either side of the deformed zone, then the deformation within must involve a stretch across the zone and/or transcurrent shear along it. We term such deformation Transpression (Fig. 1). This term was used by Harland (1971) to describe deformation arising from the oblique convergence of plates. The model has been generalized somewhat in this paper, and includes Harland's transtension.

Consider a zone within which there is no volume change and which is laterally confined (i.e. there is no stretch along the zone leading to extrusion of material at its ends). Then the shortening across the zone results in an area change which must be compensated by vertical thickening in order to conserve volume. If there is a component of shear along the zone, then the deformation can be factorized into pure shear and simple shear components as follows

$$\mathbf{D} = \begin{pmatrix} 1 & \gamma & 0 \\ 0 & 1 & 0 \\ 0 & 0 & 1 \end{pmatrix} \begin{pmatrix} 1 & 0 & 0 \\ 0 & \alpha^{-1} & 0 \\ 0 & 0 & \alpha \end{pmatrix} = \begin{pmatrix} 1 & \alpha^{-1}\gamma & 0 \\ 0 & \alpha^{-1} & 0 \\ 0 & 0 & \alpha \end{pmatrix}. \quad (1)$$

This factorization and the parameters α and γ are defined in Fig. 1, where α^{-1} specifies the shortening across the zone, α the vertical stretch and γ the shear strain parallel to the zone. More strictly α^{-1} is the ratio of the deformed to original width of the zone. Where $\gamma \neq 0$, this differs from the stretch of a line normal to the zone boundary and balancing sections across the zone should not be used to estimate α^{-1} directly.

The formulation in equation (1) is called factorization since it defines a strain in terms of two factors α and γ. The process is analogous to the factorization of matrices. Since matrix multiplication is non-commutative the sequence of multiplication in equation (1) is chosen for mathematical convenience and to give the simple definition of γ as the shear strain normal to the zone. This treatment is similar to that of Matthews *et al.* (1971, 1974). It does not necessarily imply any sequence of deformation (see later).

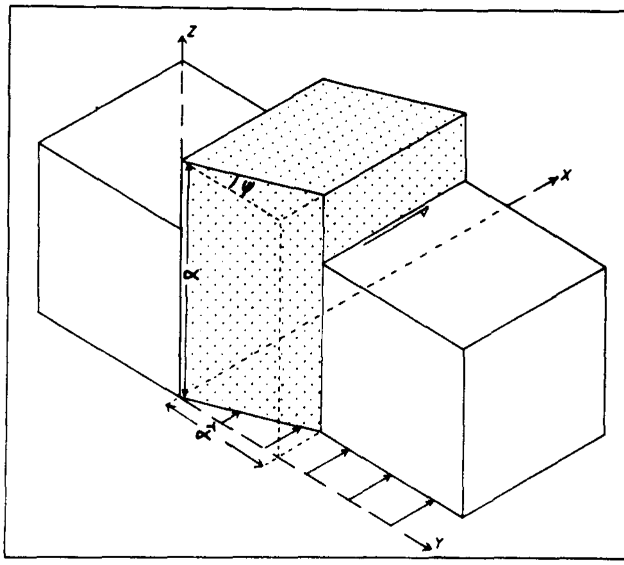

Fig. 1. Transpression geometry, showing transformation of a unit cube by shortening parallel to Y-axis and shear parallel to X-axis. Volume conserved by lengthening parallel to Z-axis.

FINITE STRAIN IN TRANSPRESSION

Strain ellipsoid

By assigning different values to the parameters α^{-1} and γ we can evaluate the finite strain, and thus learn how varying amounts of shortening and shear strain are reflected in the finite strain state of the rocks in the zone. These calculations may be done by formulating $\mathbf{D}$ and finding the eigenvalues and eigenvectors of the Finger tensor $\mathbf{DD}'$ (see Sanderson *et al.* 1980, Sanderson 1982)

SG 6:5-A

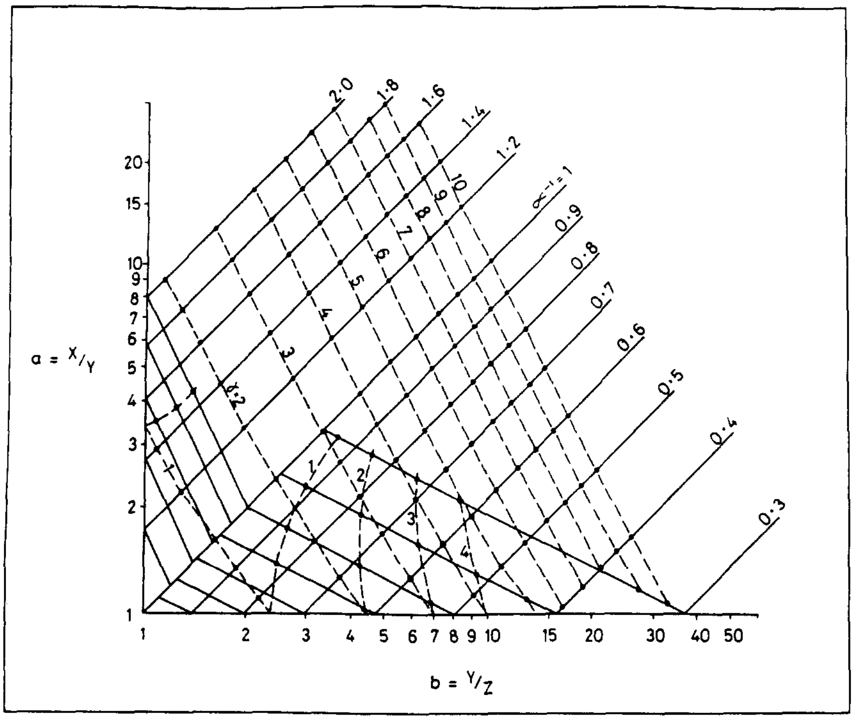

Fig. 2. Deformation plot (Flinn diagram) showing axial ratios $a = X/Y$ and $b = Y/Z$ produced by transpression model for various values of α^{-1} (continuous line) and γ (dashed line).

which give the principal quadratic elongations and principal strain axes, respectively. Figure 2 shows the finite strain grid produced.

Clearly the shape of the strain ellipsoid varies with α^{-1} as follows

for $\alpha^{-1} < 1$, oblate strains ($k < 1$) are produced;
for $\alpha^{-1} = 1$, plane strain ($k = 1$) results – simple shear;
for $\alpha^{-1} > 1$, prolate strains ($k > 1$) result.

Whilst Fig. 2 gives the shape of the strain ellipsoid there are important variations in the orientations of its principal axes ($X > Y > Z$). One principal strain is always vertical. For simple shear ($\alpha^{-1} = 1$) this is the Y-axis. For $\alpha^{-1} < 1$ the vertical axis may be either X or Y, thus the XY-plane (cleavage?) is always vertical but at an angle (θ') to the zone boundary (Fig. 3). For $\alpha^{-1} > 1$, either Z or Y may be vertical, thus the XY-plane 'switches' between vertical and horizontal. These 'switches' in principal axes occur where the strain ellipsoid assumes a $k = 0$ or $k = \infty$ shape and hence at the axes of the strain plot in Fig. 2 (see Ramsay & Wood 1973, Sanderson 1976 for discussion of similar features).

Change in angle

The transformation of a unit vector ($x = \cos\phi$, $y = \sin\phi$) is given by

$$\begin{pmatrix} x' \\ y' \end{pmatrix} = \begin{pmatrix} 1 & \alpha^{-1}\gamma \\ 0 & \alpha^{-1} \end{pmatrix} \begin{pmatrix} \cos\phi \\ \sin\phi \end{pmatrix} \quad (2)$$

which on expansion gives

$$x' = \cos\phi + \alpha^{-1}\gamma\sin\phi \quad (3a)$$
$$y' = \alpha^{-1}\sin\phi \quad (3b)$$

and therefore

$$\cot\phi' = x'/y' = (\cos\phi + \alpha^{-1}\gamma\sin\phi)(\alpha^{-1}\sin\phi)^{-1}$$
$$\cot\phi' = \alpha\cot\phi + \gamma. \quad (4)$$

This formula gives the orientation of a line after deformation in terms of the parameters α and γ, within the horizontal plane (XY of Fig. 1).

Change in length

The squared length of a transformed unit vector is the quadratic elongation (λ) and from equation (3)

$$\lambda = x'^2 + y'^2 = (\cos\phi + \alpha^{-1}\gamma\sin\phi)^2 + \alpha^{-2}\sin^2\phi$$
$$\lambda = 1 + (\alpha^{-2} + \alpha^{-2}\gamma^2 - 1)\sin^2\phi + 2\alpha^{-1}\gamma\cos\phi\sin\phi. \quad (5)$$

This expresses the quadratic elongation of a line in terms of ϕ, its orientation in the undeformed state.

To find the corresponding expression in terms of the orientation in the deformed state (ϕ') we need to consider the inverse transformation

$$\begin{pmatrix} x \\ y \end{pmatrix} = \begin{pmatrix} 1 & -\gamma \\ 0 & \alpha \end{pmatrix} \begin{pmatrix} x' \\ y' \end{pmatrix}. \quad (6)$$

The reciprocal quadratic elongation ($\lambda' = 1/\lambda$) is simply the squared length of a line before deformation which yields a unit vector afterwards, hence

$$\lambda' = x^2 + y^2 = (\cos\phi^1 - \gamma\sin\phi')^2 + \alpha^2\sin^2\phi'$$
$$\lambda' = 1 + (\alpha^2 + \gamma^2 - 1)\sin^2\phi' - 2\gamma\sin\phi'\cos\phi'. \quad (7)$$

Equations (5) and (7) reduce to those for simple shear when $\alpha = 1$ and pure shear when $\gamma = 0$.

INCREMENTAL STRAINS AND STRAIN PATHS

Figures 2 and 3 describe the finite strain fields which result from the transpression model. It must not be

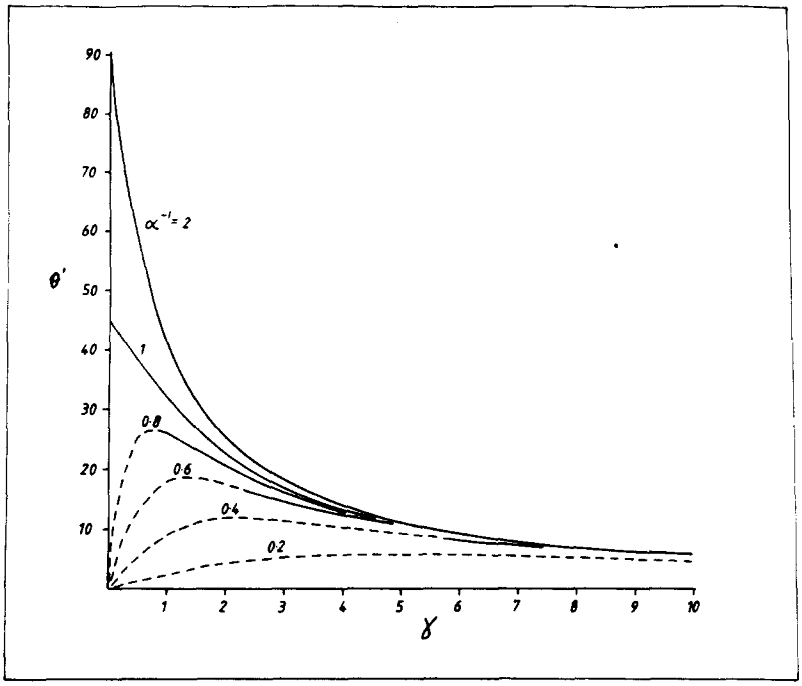

Fig. 3. Plot of orientation of long axis of strain ellipse in horizontal plane (θ'). Continuous lines indicate X-axis horizontal, dashed lines indicate X-axis vertical.

assumed that the lines on these diagrams represent deformation paths. In general any finite strain state may be reached by an infinite number of deformation paths, and it is the path (including rotation) which determines the progressive development of structures in any deformation. In order to understand the kinematics of transpression zones we need to make further assumptions about the deformation path. We will consider two special cases.

(a) *Constant incremental strain*

If we let $\gamma \rightarrow 0$ and $\alpha^{-1} \rightarrow 1$, in practice let $-0.1 < \gamma_i < 0.1$ and $0.95 < \alpha_i^{-1} < 1.05$, we define a small strain which approximates the incremental strain. A convenient parameter to specify the relative magnitudes of α_i^{-1} and γ_i is

$$T_i = \gamma_i(1 - \alpha_i^{-1})^{-1}. \quad (8)$$

Values of α_i^{-1} and γ_i are chosen to give a specific value of T_i. If both numerator and denominator of equation (8) are doubled but still produce the same deformation path then the increments are considered small enough for modelling purposes. The incremental strain matrix ($\mathbf{D}_i$) has two important modelling properties.

Firstly, by sequentially premultiplying these matrices we get a finite strain with each successive increment defining the deformation path, both in terms of the shape and orientation of the finite strain ellipsoid. We call this process powering the matrix such that $\mathbf{D} = \mathbf{D}_i^n = \mathbf{D}_i . \mathbf{D}_i . \mathbf{D}_i . . . \mathbf{D}_i . \mathbf{D}_i$. Various examples of constant incremental deformation paths are plotted in Fig. 4. One feature from these plots is that the principal axes can 'swap' along some paths of constant incremental strain (such as path 3 in Fig. 4). Also, there is a change from those with low k-values and X vertical, to higher k-values and X horizontal. Similarly for $\alpha^{-1} > 1$, very high k-values accompany vertical Z-axes. The axis swapping is very interesting since it indicates that the maximum finite stretch may be normal to the maximum incremental stretch. Thus the geometrical relationships between structures related to finite strain (cleavage and stretching lineations) and those related to incremental strain (fractures, etc.) may be complex.

Secondly, the incremental strain axes will be parallel to the principal stresses, thus we can predict the orientation of failure in the zone (at least if we assume it is elastically isotropic). Figure 5 shows the influence of α^{-1} on the orientation of maximum compression axes and the sorts of structures which might result. These diagrams include as a special case ($\alpha^{-1} = 1$) the well known wrench tectonics patterns of Moody & Hill (1956) and Wilcox *et al.* (1973).

Some important features of transpression are obvious from Fig. 5. The 45° obliquity of structures in simple shear zones (see Ramsay & Graham 1970, Ramsay 1980) is modified. For $\alpha^{-1} < 1$, folds and thrusts initiate at much lower angles to the zone, whereas extensional structures (veins, dykes, normal faults, etc.) initiate at higher angles. The opposite applies where $\alpha^{-1} > 1$. Subsequent rotation as strain progresses will also modify these directions as in simple shear, but this is now governed by equation (4). In applying these concepts it must be remembered that transpression requires a strain discontinuity or zone of complex strain between the interior and exterior of the zone. For this reason simple shear may be fairly common in nature, especially where zones remain continuous with undeformed rock. Volume change, however, may occur, in which case α^{-1} represents the dilation $(1 + \Delta)$ of Ramsay & Graham (1970) in equations (2)–(7). Thus the two-dimensional,

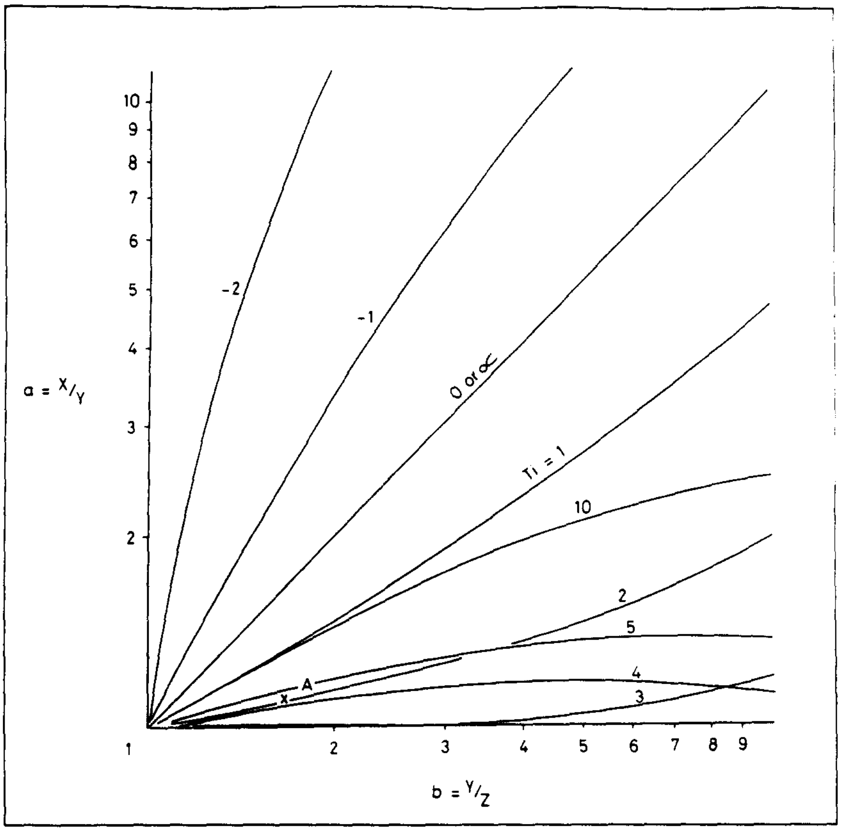

Fig. 4. Constant incremental strain paths for the transpression model. Values on paths are numerical labels derived by dividing incremental shear strain by $(1 - \alpha_i^{-1})$. Note the 'swapping' of axes indicated by 'bouncing' of strain path off the b-axis for path number 3.

but not three-dimensional, aspects of the model may be applied to volume change and the patterns in Fig. 5 obtained.

(b) *Simple Transpression (as defined by Harland* 1971)

In general we cannot predict deformation paths with any degree of certainty, although the use of incremental strain indicators (Elliott 1972) may constrain the choice. If the stresses and material properties of the rock remain constant, then we might predict constant strain increments, but clearly these situations are unlikely to apply to natural deformation. Arguments based on the minimum work principle (Nadai 1963) seem equally impractical since they require the rock to prejudge its final strain state and be able to compute the required strains. Deformation paths are more probably determined by two main factors, the external boundary displacements of the system and the internal rheological variations of which layering is a common and important geological example. The latter are difficult to treat and the former usually impossible to specify.

Harland (1971) suggested a form of deformation which he called Simple Transpression in which he specified the deformation in terms of a set of boundary conditions involving two rigid boundaries approaching one another obliquely (Fig. 6). If we assume that the material is isotropic we can determine the finite strain at various increments of shortening (S) and hence define the deformation path relative to this time-like parameter.

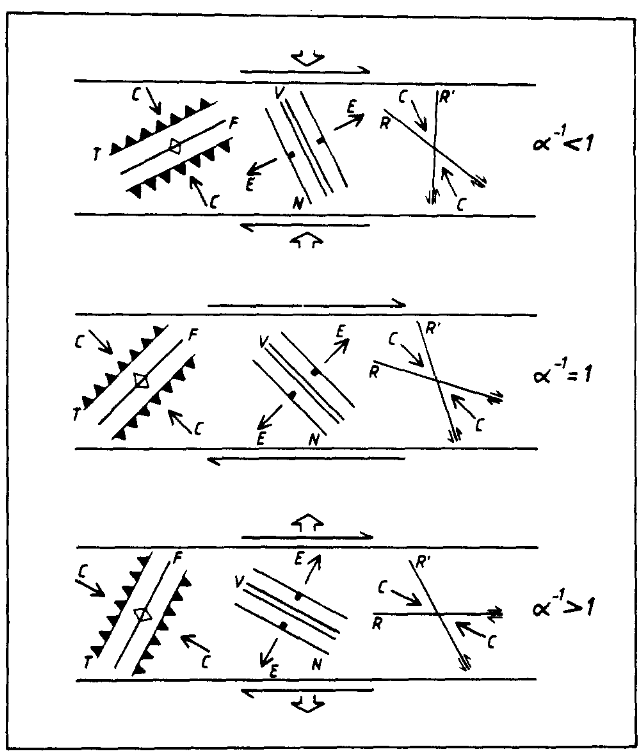

Fig. 5. Diagrams to show orientations of fractures in the transpression model. C, 'compression axis' (σ_1); E, 'extension axis' (σ_3); N, normal faults; T, thrust faults; R, R', Riedel shears or wrench faults; V, veins, dykes or extension fractures; F, fold axes. The central diagram corresponds to the classical Wrench tectonics model.

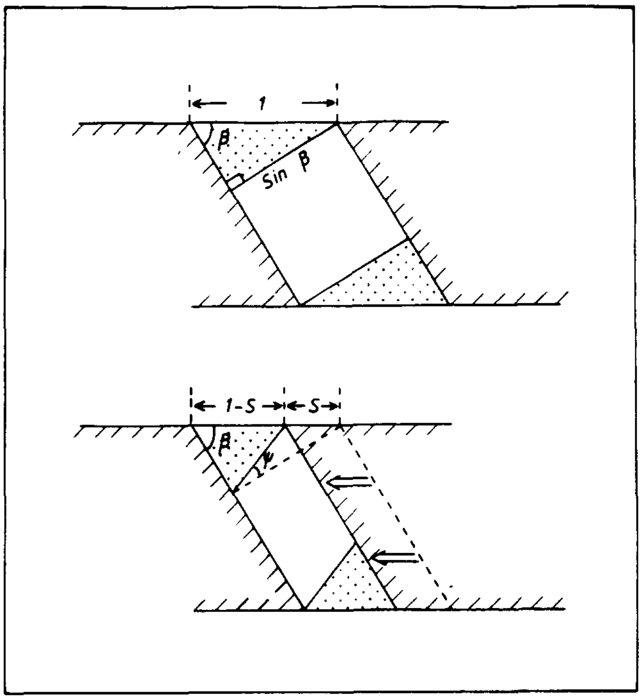

Fig. 6. Simple Transpression model involving movement of rigid blocks (diagonal shading) with transpressive deformation of stippled zone. For further discussion see text.

The shortening across the zone is given by

$$\alpha^{-1} = (1 - S)$$

and from Fig. 6

$$\frac{S}{\sin \psi} = \frac{\sin \beta}{\sin (90 + \beta - \psi)} = \frac{\sin \beta}{\cos (\beta - \psi)}$$

$$= \frac{\sin \beta}{\cos \beta \cos \psi + \sin \beta \sin \psi}$$

from which

$$\gamma = \tan \psi = S(1 - S)^{-1} \cot \beta.$$

Thus, α^{-1} and γ can be expressed in terms of S for any given value of β. Figure 7 shows the deformation paths for various values of β.

This special case has been analysed to show how one might approach problems from a knowledge or assumption of the boundary conditions. The model itself might be used to simulate the oblique collision of two continents or the oblique closure of a basin. It also illustrates the important philosophical point that even simple boundary conditions can give rise to quite complex deformation paths. In this case where β is small the deformation path contains a switching of the X and Y axes (Fig. 7).

APPLICATION OF THE TRANSPRESSION MODEL TO ZONES OF FOLDING

The purpose of this section is to examine the use of the transpression model in the interpretation of fold patterns. Since many factors influence fold development it is not intended that fold patterns should be used to evaluate the strain parameters, but simply to see if reasonable parameters give rise to observed patterns.

(a) *En-échelon folding*

En-échelon folding has often been attributed to wrench tectonics, and simple shear used to conceptualize its development (Moody & Hill 1956, Moody 1973, Harding 1973, 1974, Wilcox *et al.* 1973). In simple shear the incremental minimum stretch (Z_i) is at 45° to the shear plane, and hence folds would be expected to initiate normal to this direction (Fig. 5b). Almost all the examples in the works listed above have folds at angles ≤45° to the zones. For example, Moody & Hill (1956) summarize folds from southern California and conclude that they trend at <25° to the known wrench faults.

It is true that the fold axes may rotate towards the shear plane with increasing strain, but high shear strain ($\gamma > 2$) is necessary to reduce this angle to <22.5°. Such shear strains imply considerable shortening across the folds (*c.* 60% for $\gamma = 2$), which greatly exceeds likely values in these areas.

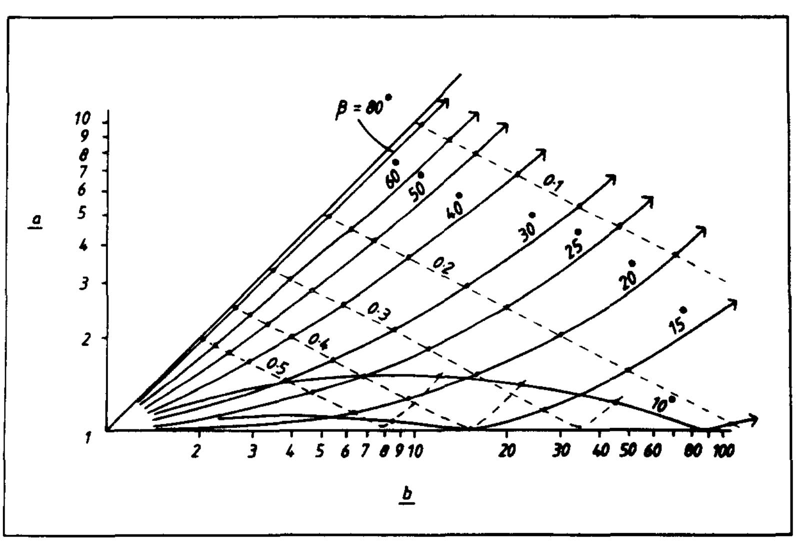

Fig. 7. Strain paths for Simple Transpression model. Continuous lines are strain paths for labelled β angles, dashed lines indicate amount of shortening across zone (α^{-1}), $a = X/Y$, $b = Y/Z$.

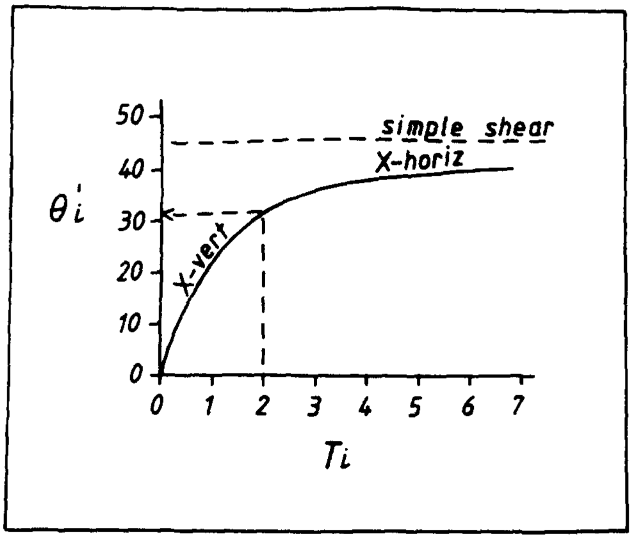

Fig. 8. Initial angle (θ_i') of strike of maximum incremental stretch in horizontal plane for different incremental strains (T_i).

The transpression model, however, allows fold initiation at angles <45°. Figure 8 shows the angle of initiation (θ_i') for different values of T_i. For example, consider increments $\alpha_i^{-1} = 0.99$, $\gamma_i = 0.02$, i.e. $T_i = 2$, in the incremental strain matrix, this produces Z_i at *c.* 59° to the zone. Thus the model predicts fold initiation at *c.* 31° to the zone.

(b) *Obliquity of major and minor folds*

To model the progressive development of folds let us consider what might happen as en-échelon folds develop. Using the previous example of a fold initiating at *c.* 31° in a zone with $T_i = 2$, we can power the incremental strain matrix $\mathbf{D}_i$ to give us the constant increment deformation path (Fig. 4) and from it find the values of α^{-1} and γ at any stage in the deformation. Let us consider the point A in Fig. 4 where the values are $\alpha^{-1} = 0.8$, $\gamma = 0.5$. Since the fold axis initiated at $\theta_i' = 31°$ to the zone, and assuming passive rotation, we may use equation (4) to calculate that it will rotate to an angle $\theta_i' = 21°$.

Thus the early formed folds rotate and tighten, but for constant incremental strain any newly formed folds will still initiate on flat lying beds at $\theta_i' = 31°$. The net result will be the development of a pattern of folding with early major folds at *c.* 21° to the zone and with gentle minor folds on their shallow dipping limbs or hinge zones at a higher angle (*c.* 31°) to the zone.

This pattern of minor folds oblique to major folds has been seen in strike-slip zones. Figure 9 shows an example from the aureole of the Main Donegal granite, Ireland. Hutton (1982) describes how minor folds (locally F_4, regionally F_6) and a crenulation cleavage initiate at *c.* 45° to a shear zone and rotate into parallelism with it as the strain increases. This and other strain features (see also Sanderson *et al.* 1980), are attributed to left-lateral shear. The figured fold comes from near the edge of the zone and clearly shows minor folds in the hinge region of a larger antiform. The minor folds trend clockwise of the major hinge, this being consistent with left-lateral shear.

Similar obliquity of gentle minor folds to open/close major folds has been found by the authors in another left-lateral zone in the Slick Hills, which form part of the southern Oklahoma aulacogen, between the Wichita uplift and the Anadarko basin. Arthurton (1983) describes similar obliquity in the Skipton area, northern England, in a region of right-lateral wrench tectonics. The obliquity of major and minor folds might present a useful indicator of strike-slip components of deformation.

TRANSPRESSION AT BENDS AND TERMINATIONS

As with the wrench tectonics model, departures from parallel-sided deformation zones, such as offsets and changes in zone width, will introduce added complexity to the model and the resulting deformation patterns.

(a) *Bends producing oblique convergence*

Even in the absence of a shear component along the zone (i.e. $\gamma = 0$), offsets will produce en-échelon patterns of folds (Fig. 10). The offset may be modelled by Simple Transpression and from the angle (β), the fold axis orientation predicted. In Fig. 10, with $\beta = 45°$, folds initiate at *c.* 22° to the offset boundary and produce an en-échelon array with individual folds at *c.* 67° to the array.

(b) *Bends in simple shear zones*

In a simple shear zone the Simple Transpression model can also be used to model bend strains (Fig. 11). If we have rigid blocks bounding the offset zone then simple shear along the overall zone induces Simple Transpression in the offset zone. As with wrench tectonic models, the sense of offset determines whether the zones are 'compressive' ($\alpha^{-1} < 1$) or 'dilational' ($\alpha^{-1} > 1$).

For 'compressive' offsets (Fig. 11) transpression produces folds at a high angle to the overall zone and the 'compression' will be accommodated by crustal thickening (i.e. $\alpha > 1$). This in turn produces uplift and the boundaries between the transpression region and the rest of the shear zone may develop as high-angle reverse, or oblique-slip, faults (Fig. 11). These uplifted regions will also be areas of more intense strain.

When 'dilational' offsets develop (Fig. 11), $\alpha < 1$ and crustal thinning results. Extensional features such as dykes, normal faults and veins will be oriented at a high angle to the shear zone, and any folds will be at a low angle. The crustal thinning will produce subsidence and the development of pull-apart basins.

Where offsets are numerous and complex a braided fault zone may develop. This will be characterized by juxtaposed basins and uplifts. The basins should have folds sub-parallel to the zone and have many diagonal or

Fig. 9. Example of oblique development of minor folds in hinge of major fold from the aureole of the Main Donegal granite Ireland.

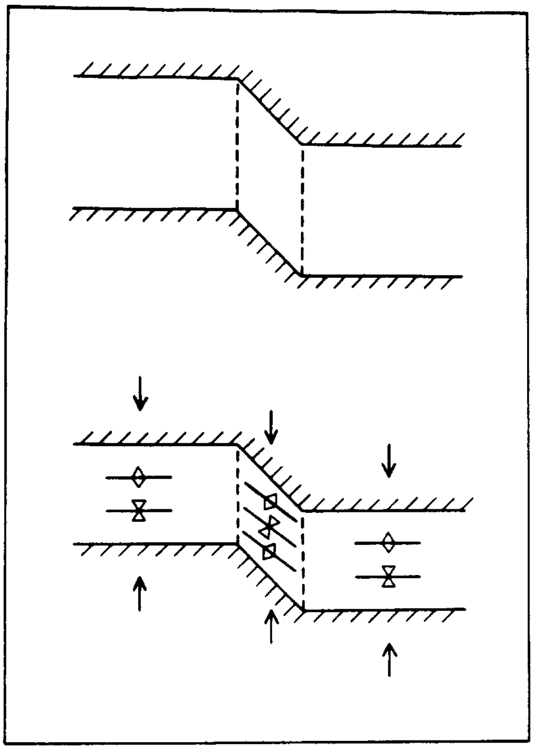

Fig. 10. Model to show generation of transpressive region between offset in a compression zone ($\gamma = 0$). Shortening, $\alpha^{-1} = 0.8$ in lower diagram.

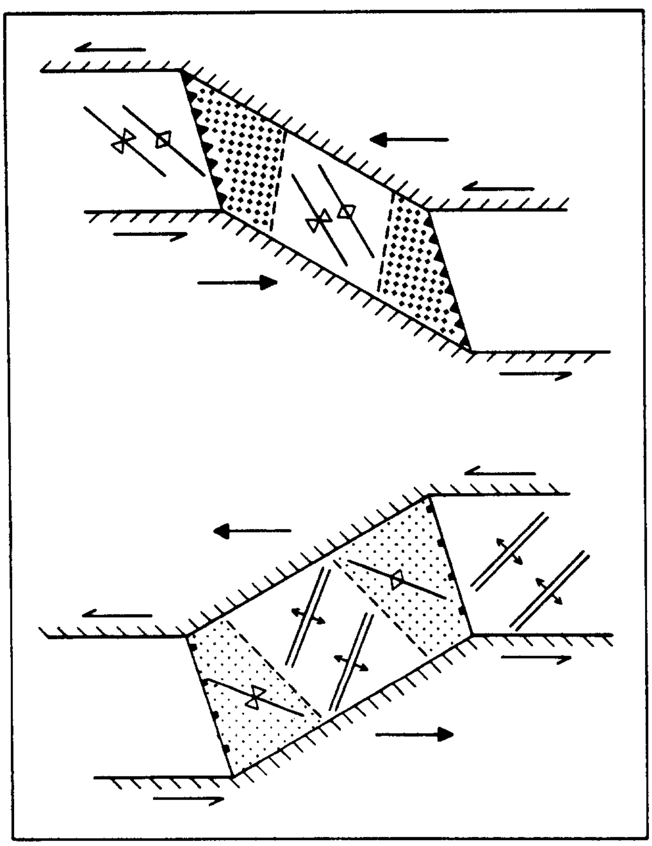

Fig. 11. Diagram to show generation of a Simple Transpressive zone in a region of offset of a shear zone (i.e. simple shear). The upper rigid block (diagonal shading) moves left relative to the lower one, generating the area of transpression (dots and crosses). The unshaded parts of the zone undergo simple shear. Orientation of fold axes inside and outside the transpression region are shown. The boundaries between the vertically thickened (crosses) or thinned (stippled), transpressive regions and those of simple shear (unchanged thickness) are shown as faults, necessary to accommodate the strain discontinuity between the two.

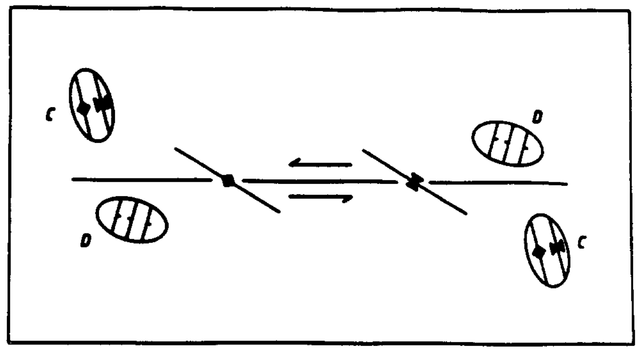

Fig. 12. Pattern of strain distribution in 'transpression' regions at terminations of wrench faults. *C*, compression zones showing fold orientations; *D*, dilation zones showing normal fault orientations.

cross faults with normal or oblique-slip movement. The uplifts might be expected to be dominated by folds and reverse faults, which initially developed at a high angle to the zone but may be subsequently rotated if the strain is large. Faults would be diagonal or longitudinal to the folding.

Many of these characteristics can be seen in the San Andreas fault zone (e.g. Harding 1974, and particularly, Sylvester & Smith 1976) and in the Najd fault system, Saudi Arabia (Moore 1979).

(c) *Terminations of wrench zones*

Terminations are much the same as offsets; they give rise to localized compression and dilation zones (Fig. 12). The boundary conditions are more complex since they have only one bounding fault. They would be expected to give rise to similar patterns of structures and localized uplift and subsidence. Compressive regions should be characterized by folds and reverse faults at a high angle to the zone, whereas dilational zones would have normal faults at a high angle and folds at a low angle to the zone. Patterns of this sort are clearly seen in the Najd fault system (Moore 1979).

NEAR-SURFACE EFFECTS OF TRANSPRESSION

One important aspect of the transpression model, which differs from wrench-type simple shear, is the vertical stretch (α). This may involve either thickening ($\alpha > 1$) or thinning ($\alpha < 1$) of the zone. Thus transpression operating over substantial crustal thicknesses involves uplift or subsidence of the surface. As we have seen from the previous section, this may be most marked at offsets and terminations of faults, but it could also be a general feature of the entire zone.

One of the best documented examples of the vertical displacements associated with transpression is in a study of the Mecca anticline in the San Andreas fault zone by Sylvester & Smith (1976). They describe a zone of shortening and uplift, bounded by convex-upward faults, that is curved faults which steepen downwards. These faults have a combination of reverse and strike-slip displacement. On either side of the block they dip

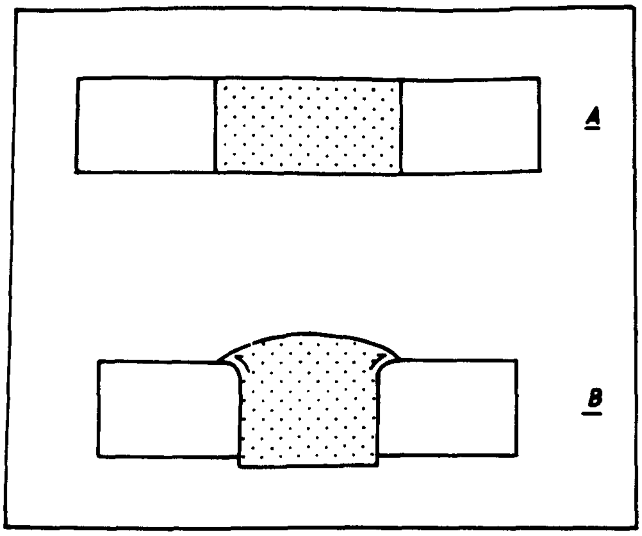

Fig. 13. Diagrammatic cross-section of a transpression zone showing crustal thickening and development of 'flower structure'.

inward, producing a wedge-shaped or 'keystone' uplift (Fig. 13). Similar structures are common in seismic sections of wrench zones and are termed 'flower structure' (Harding & Lowell 1979). Gravitational collapse and/or gliding at the margins of the uplifted block may produce structures typical of thrust tectonic regimes.

CONCLUSIONS

Transpression represents a model with which to interpret structural features within fault-bounded zones of deformation. It involves a combination of pure shear and simple shear, both of which occur as special cases ($\gamma = 0$ and $\alpha = 1$, respectively).

Crustal shortening ($\alpha > 1$) and wrench-type shear produce:

(1) flattening (oblate) strain ($k < 1$),

(2) steep cleavage and a stretching lineation which may be either vertical or horizontal,

(3) folds and thrusts at small oblique angles to the zone,

(4) normal faults, dykes, veins and other extensional structures at a high angle to the zone and

(5) crustal thickening and vertical uplift.

Crustal extension and shear ('transtension' of Harland 1971) produce:

(1) constrictional (prolate) strain ($k > 1$),

(2) horizontal stretching, with steep or flat cleavage,

(3) folds and thrusts at a high angle to the zone,

(4) extensional structures at a low angle and

(5) crustal thinning, subsidence and basin development.

Whilst this type of deformation can be applied to the bulk strain in entire zones, it is also useful in interpreting offsets and terminations in wrench zones and in describing the strain in any block of crust defined by a parallelogram of faults.

The bounding faults are important, since strain is not compatible between undeformed rock and that undergoing transpression. In general these bounding faults will be steep, oblique-slip faults, but they may flatten upward. They typically dip in under uplifted blocks producing a 'flower structure'.

Acknowledgements—We wish to thank Nowell Donovan for introducing us to the problems of wrench tectonics in southern Oklahoma and for help and discussion of our work there. One of us (W.R.D.M.) acknowledges a grant from the Department of Education, Northern Ireland.

REFERENCES

Arthurton, R. S. 1983. The Skipton Rock Fault—an Hercynian wrench fault associated with the Skipton Anticline, northwest England. *Geol. J.* **18**, 105–114.

Elliott, D. 1972. Deformation paths in structural geology. *Bull. geol. Soc. Am.* **83**, 2621–2638.

Harding, T. P. 1973. The Newport–Inglewood trend, California—an example of wrenching style of deformation. *Bull. Am. Ass. Petrol. Geol.* **57**, 97–116.

Harding, T. P. 1974. Petroleum traps associated with wrench faults. *Bull. Am. Ass. Petrol. Geol.* **58**, 1290–1304.

Harding, T. P. & Lowell, J. D. 1979. Structural styles, their plate tectonic habitats, and hydrocarbon traps in petroleum provinces. *Bull. Am. Ass. Petrol. Geol.* **63**, 1016–1058.

Harland, W. B. 1971. Tectonic transpression in Caledonian Spitsbergen. *Geol. Mag.* **108**, 27–42.

Hutton, D. H. W. 1982. A tectonic model for the emplacement of the Main Donegal Granite, NW Ireland. *J. geol. Soc. Lond.* **139**, 615–631.

Matthews, P. E., Bond, R. A. B. & Van den Berg, J. J. 1971. Analysis and structural implications of a kinematic model of similar folding. *Tectonophysics* **12**, 129–154.

Matthews, P. E., Bond, R. A. B. & Van den Berg, J. J. 1974. An algebraic method of strain analysis using elliptical markers. *Tectonophysics* **24**, 31–67.

Moody, J. D. 1973. Petroleum exploration aspects of wrench-fault tectonics. *Bull. Am. Ass. Petrol. Geol.* **57**, 449–476.

Moody, J. D. & Hill, M. J. 1956. Wrench-fault tectonics. *Bull. geol. Soc. Am.* **57**, 1207–1246.

Moore, J. McM. 1979. Tectonics of the Najd transcurrent fault system, Saudi Arabia. *J. geol. Soc. Lond.* **136**, 441–454.

Nadai, A. 1963. *Theory of Flow and Fracture of Solids.* Vol. 2. McGraw-Hill, New York.

Ramsay, J. G. 1980. Shear zone geometry: a review. *J. Struct. Geol.* **2**, 83–99.

Ramsay, J. G. & Graham, R. H. 1970. Strain variation in shear belts. *Can. J. Earth Sci.* **7**, 786–813.

Ramsay, J. G. & Wood, D. S. 1973. The geometric effects of volume change during deformation processes. *Tectonophysics* **16**, 263–277.

Sanderson, D. J. 1976. The superposition of compaction and plane strain. *Tectonophysics* **30**, 35–54.

Sanderson, D. J. 1982. Models of strain variation in nappes and thrust sheets: a review. *Tectonophysics* **88**, 201–233.

Sanderson, D. J., Andrews, J. R., Phillips, W. E. A. & Hutton, D. H. W. 1980. Deformation studies in the Irish Caledonides. *J. geol. Soc. Lond.* **137**, 289–302.

Sylvester, A. G. & Smith, R. R. 1976. Tectonic transpression and basement-controlled deformation in San Andreas fault zone, Salton trough, California. *Bull. Am. Ass. Petrol. Geol.* **60**, 2081–2102.

Wilcox, R. E., Harding, T. P. & Seely, D. R. 1973. Basic wrench tectonics. *Bull. Am. Ass. Petrol. Geol.* **57**, 74–96.